



# Adjuvant Potential of Poly- $\alpha$ -L-Glutamine from the Cell Wall of *Mycobacterium tuberculosis*

Rajesh Mani,<sup>a,c</sup> Manish Gupta,<sup>a</sup> Anshu Malik,<sup>a</sup> Ravi Tandon,<sup>b</sup> Rajendra Prasad,<sup>c</sup> Rakesh Bhatnagar,<sup>a</sup> Nirupama Banerjee<sup>a</sup>

<sup>a</sup>Molecular and Cell Biology Laboratory, School of Biotechnology, Jawaharlal Nehru University, New Delhi, India

<sup>b</sup>Laboratory of AIDS Research and Immunology, School of Biotechnology, Jawaharlal Nehru University, New Delhi, India

<sup>c</sup>Amity Institute of Biotechnology, Amity University, Amity Education Valley, Gurgaon, Haryana, India

**ABSTRACT** Novel adjuvants are in demand for improving the efficacy of human vaccines. The immunomodulatory properties of *Mycobacterium tuberculosis* cell wall components have been highlighted in the formulation of complete Freund's adjuvant (CFA). We have explored the adjuvant potential of poly- $\alpha$ -L-glutamine (PLG), a lesser-known constituent of the pathogenic mycobacterial cell wall. Immune parameters indicated that the adjuvant potency of PLG was statistically comparable to that of CFA and better than that of alum in the context of H1 antigen (Ag85B and ESAT-6 fusion). At 1 mg/dose, PLG augmented the immune response of Ag85B, BP26, and protective antigen (PA) by increasing serum antibodies and cytokines in the culture supernatant of antigen-stimulated splenocytes. PLG modulated the humoral response of vaccine candidate ESAT-6, eliciting significantly higher levels of total IgG and isotypes (IgG1, IgG2a, and IgG2b). Additionally, the splenocytes from PLG-adjuvanted mice displayed a robust increase in the Th1-specific gamma interferon, tumor necrosis factor alpha, interleukin-2 (IL-2), Th2-specific IL-6 and IL-10, and Th17-specific IL-17A cytokines upon antigenic stimulation. PLG improved the protective efficacy of ESAT-6 by reducing bacillary load in the lung and spleen as well as granuloma formation, and it helped in maintaining vital health parameters of mice challenged with *M. tuberculosis*. The median survival time of PLG-adjuvanted mice was 205 days, compared to 146 days for dimethyl-dioctadecyl ammonium bromide-monophosphoryl lipid A (DDA-MPL)-vaccinated groups and 224 days for *Mycobacterium bovis* BCG-vaccinated groups. PLG enhanced the efficiency of the ESAT-6 vaccine to the level of BCG and better than that of DDA-MPL ( $P < 0.05$ ), with no ill effect in C57BL/6J mice. Our results propose that PLG is a promising adjuvant candidate for advanced experimentation.

**KEYWORDS** *Mycobacterium tuberculosis* H37Rv, cell wall, adjuvants, poly- $\alpha$ -L-glutamine, Th1/Th2/Th17 responses, ESAT-6, vaccines

According to a recent 2017 World Health Organization report, tuberculosis (TB) has emerged as the foremost cause of worldwide mortality, with about 10.4 million new cases and 1.3 million deaths in 2016 (1). Since 1921, *Mycobacterium bovis* bacillus Calmette-Guérin (BCG) remains the only available vaccine against TB, with protective efficacy from 0 to 85%. Although BCG has been successfully employed worldwide to prevent the disease in infants, it is ineffective in adolescents and adults against pulmonary TB (2). The emergence of multidrug-resistant (MDR) and extensively drug-resistant (XDR) strains has prompted an urgent need for development of an improved and efficient TB vaccine (3).

Traditionally, live attenuated and inactivated pathogens have been used for vaccination, but due to several shortcomings, e.g., reactogenicity, insufficient potency and efficacy, reversion of live-attenuated strains to virulence due to incomplete inactivation

Received 12 July 2018 Returned for modification 24 July 2018 Accepted 5 August 2018

Accepted manuscript posted online 13 August 2018

**Citation** Mani R, Gupta M, Malik A, Tandon R, Prasad R, Bhatnagar R, Banerjee N. 2018. Adjuvant potential of poly- $\alpha$ -L-glutamine from the cell wall of *Mycobacterium tuberculosis*. *Infect Immun* 86:e00537-18. <https://doi.org/10.1128/IAI.00537-18>.

**Editor** Sabine Ehrh, Weill Cornell Medical College

**Copyright** © 2018 American Society for Microbiology. All Rights Reserved.

Address correspondence to Nirupama Banerjee, [nirupamaban@yahoo.com](mailto:nirupamaban@yahoo.com).

R.M. and M.G. contributed equally to this work.

of the organism, etc., their usage in humans is limited (4). Many of the modern-day vaccines contain highly purified recombinant antigens or their peptide derivatives with minimum toxicity and good safety profiles, and they are preferred over traditional whole-cell vaccines (5). However, the recombinant purified antigens alone are often associated with poor immunogenicity compared to live attenuated vaccines, and additional supplements are needed to augment the immune response of the antigen. One such component is an adjuvant known to augment the antigen-specific immune response in the host (6). The adjuvants are defined as the compounds that can enhance and/or modulate immunogenicity of a vaccine candidate intrinsically (5). Classically, an adjuvant acts as a delivery vehicle for efficient, slow, and sustained release of a vaccine antigen to the antigen-presenting cells (APCs), as an immune stimulator, or as an inducer of CD8<sup>+</sup> cytotoxic T-lymphocyte (CTL) responses (7). The immunization of purified protein antigens with adjuvants improves the quality of the vaccine in different ways, e.g., dose sparing, reduced number of immunizations, rapid response to pathogens, response broadening, effective T-cell response, etc. (5). Thus, formulation of a vaccine with a suitable adjuvant is an essential step in vaccine development for inducing sufficient protective and long-term memory response in humans (8).

The T helper 2 (Th2)-promoting aluminum salts and oil-in-water emulsion of MF59 are among the few adjuvants approved for human use that primarily induce humoral immune response (9, 10). However, Th1 response-promoting adjuvants approved for human use are scarce (11). In the cases of many deadly intracellular pathogens, like *Mycobacterium tuberculosis*, *Salmonella enterica* serovar Typhimurium, *Listeria monocytogenes*, *Brucella abortus*, etc. (12–15), the Th1-dependent immune response plays a critical role in protective immunity. Although a number of Th1 response-promoting adjuvants are being evaluated in clinical trials for human use, none of them have been approved yet (16). Thus, identification of Th1 response-promoting adjuvants for human use is highly desirable.

The only vaccine currently available against TB for humans is an attenuated strain of *Mycobacterium bovis*, called BCG (17). However, protective efficacy of BCG is inadequate against pulmonary TB in adults. Hence, it is imperative to develop an improved vaccine to combat the global threat of tuberculosis (18). Different strategies have been adopted to improve efficacy of BCG, e.g., viable attenuated, viral-vectored, inactivated whole-cell, and subunit vaccines with novel adjuvants (19). Among these strategies, subunit vaccination bears a number of advantages, such as stability, relatively lower toxicity, increased safety, and boosting effect after BCG vaccination (20).

The efficacy of a subunit vaccine is highly dependent on the choice of an effective adjuvant (21). The adjuvant property of mycobacterial cell wall components is well known (11). Complete Freund's adjuvant (CFA), a water-in-oil emulsion of killed mycobacterial cells, is one of the most commonly used adjuvants in laboratory studies and is known to induce both Th1 and Th2 immune responses. The bioactivity of CFA is attributed to *N*-acetylmuramyl-L-alanyl-D-isoglutamine (muramyl dipeptide; MDP) and trehalose 6,6'-dimycolate (TDM) (22, 23). Although widely used in animal models, CFA cannot be used in humans due to its toxicity (24) and lack of information regarding the immunostimulatory role of individual bioactive components. The adjuvant properties of some highly abundant mycobacterial cell wall components, such as TDM, lipoarabinomannan (LAM), and mycolic acids (MA), have been studied extensively (22, 25, 26), but the nature of others, like cell wall-associated polypeptides, has yet to be explored. Trehalose-6,6'-dibehenate (TDB), a synthetic analog of TDM or cord factor, is currently in phase I clinical trials as an adjuvant (27).

The glutamine-rich self-assembling peptides and peptide derivatives have emerged as promising candidates over the past 2 decades for their biomedical applications, including regenerative medicine, tissue engineering, matrices for cell culture, and adjuvants for vaccines (28). Rudra et al. reported that mice vaccinated with glutamine-rich self-assembling peptide Q11 linked to ovalbumin (OVA) induced IgG1, IgG2, IgG3, and IgM antibody titers comparable to those with CFA (28). The cell wall of *M. tuberculosis* contains poly- $\alpha$ -L-glutamine (PLG) peptides associated with the underlying

peptidoglycan layer through noncovalent interactions (29). Phiet et al. reported the presence of PLG in virulent *M. tuberculosis* and in multiple strains of BCG, as well as its absence from nonpathogenic mycobacteria like *Mycobacterium smegmatis* (30). The glutamine residues are linked through  $\alpha$ -linkage, and partial amidation of isolated polypeptide has been established earlier (31). The PLG accounts for  $\sim$ 10% of the deproteinized, delipidated cell wall of *M. tuberculosis*, while the cell wall of BCG contains  $\sim$ 2% of the polypeptide (29, 32). In pathogenic *M. tuberculosis* and *M. bovis* strains, synthesis of PLG was shown to be dependent on the presence of extracellular glutamine synthetase (eGS; encoded by the *glnA1* gene) (33, 34). Earlier we have shown that the presence of eGS and PLG in the cell wall was linked to survival and pathogenicity of *M. tuberculosis* and *M. bovis* (34, 35).

In this study, we set out to explore the adjuvant potential of PLG isolated from the cell wall of *M. tuberculosis*. In view of its inert and polymeric nature, we were motivated to investigate the biological properties of this molecule. Here, we present data comparing the adjuvant properties of PLG with the other commercially available adjuvants in the context of different antigens. Our results show that PLG was able to enhance the antigen-specific immune response and provide better protective immunity in the mouse model than other well-known adjuvants tested. A strong Th1-specific immune response triggered by *M. tuberculosis* PLG makes it a promising adjuvant candidate for the development of effective vaccines essentially against infections caused by intracellular pathogens.

## RESULTS

**Chemical and physical characterization of PLG.** The purity of PLG was increased by treatment of *M. tuberculosis* cell wall fractions with trypsin and chymotrypsin before extraction with SDS. Subsequently, acetone and chloroform-methanol (2:1) washing removed the residual SDS along with the protein and lipid impurities (for details, see Materials and Methods). The yield of pure PLG obtained after Percoll-gradient centrifugation was 16 mg/g dry weight of the cells and contained minor impurities of protein (1.55  $\mu$ g), carbohydrates (0.59  $\mu$ g), lipids ( $<$ 1  $\mu$ g), and nucleic acids ( $<$ 2  $\mu$ g) per milligram of dry weight of PLG. Gas chromatography-mass spectrometry (GC-MS) analysis of the purified PLG is shown in Fig. 1A. The minor peaks observed in the GC-MS chromatogram identified through the existing database available from the NIST 05 (National Institute of Standards and Technology) and WILEY8 chemical libraries appear to be generated during the derivatization process and are shown in Table S2 in the supplemental material. The heptafluorobutyryl-isobutyl derivative of glutamic acid (corresponding to PLG) showed a major peak with retention time of 18.821 and area of 64.96%. The purified PLG is a mixture of polypeptides of various lengths, which resolved by SDS-PAGE as a smear of high-molecular-weight aggregates to smaller peptides (Fig. 1B) and reacted with anti-polyglutamine monoclonal antibody in Western blotting (Fig. 1B). The PLG preparation is sensitive to nonspecific proteases, like proteinase K, which degraded it slowly (data not shown). The water-insoluble PLG aggregates appeared as amorphous clusters of small globular entities of an average size of  $\sim$ 23.14 nm under the transmission electron microscope (Fig. 1C). The solubility profile of PLG showed that the polypeptide is highly soluble in trifluoroacetic acid (TFA), dimethyl sulfoxide (DMSO), and sodium hydroxide (NaOH) and less soluble in organic solvents like methanol, ethanol, chloroform, and diethyl ether (Fig. 1D).

**Adjuvant properties and dose optimization of PLG.** We have evaluated the adjuvant properties of PLG peptides isolated from the cell wall of *M. tuberculosis* H37Rv for modulation of immune responses against H1 antigen vaccination and compared them with properties of two widely used adjuvants, CFA and alum. To assess the adjuvant potential, we immunized mice with immunogenic fusion antigen H1 alone or in combination with PLG (Fig. 2A). It was observed that H1 antigen or PLG alone failed to elicit any significant IgG response at 3 weeks postimmunization (Fig. 2B), but when used together, PLG augmented the IgG antibody response of H1 antigen considerably (Fig. 2B). The PLG-mediated increases in anti-H1 IgG titers were comparable to the

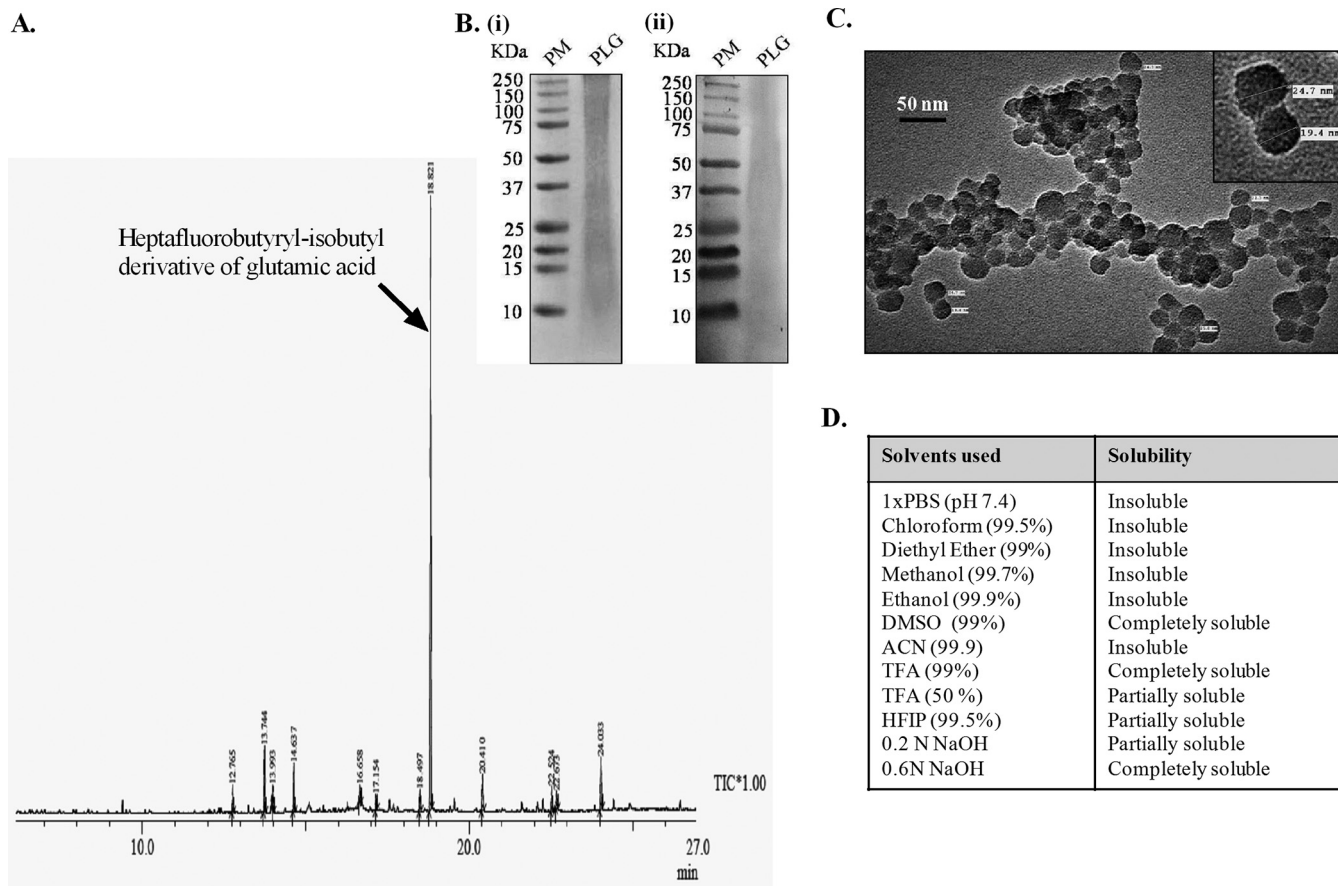
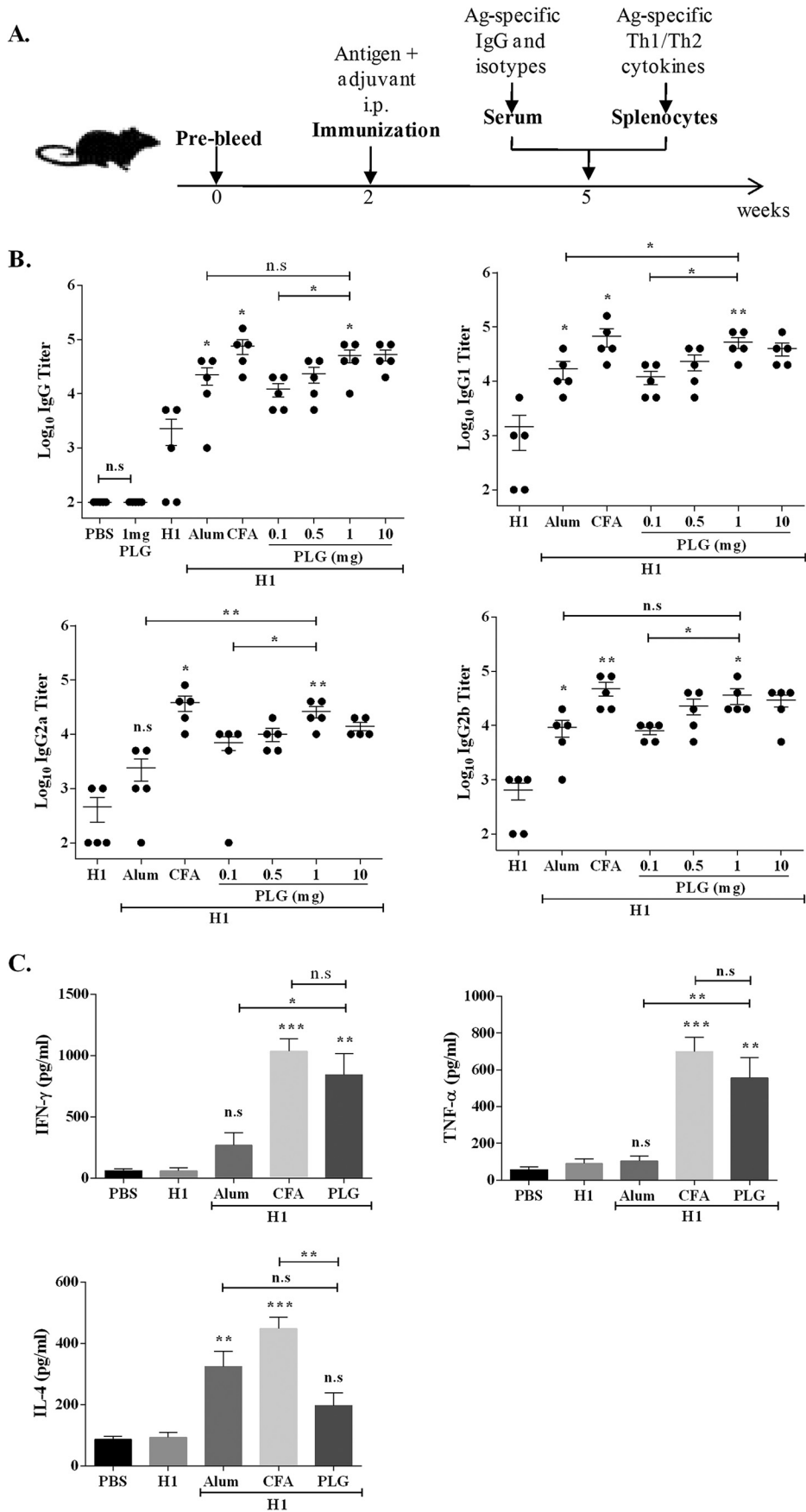


**FIG 1** Chemical and physical characterization of PLG isolated from *M. tuberculosis* cell wall. (A) GC-MS chromatogram of the PLG peptides. The arrow indicates the heptafluorobutyryl-isobutyl derivative of glutamic acid. Rt, retention time. (B) Tricine SDS-PAGE (i) and immunoblot analysis (ii) of PLG. For immunoblotting, primary antipolyglutamine monoclonal antibodies were employed. PM, Precision Plus protein standards. (C) TEM micrographs of purified PLG. The inset displays the same at higher magnification. (D) Table shows the solubility profile of *M. tuberculosis* PLG in various organic and inorganic solvents.

levels induced by alum or CFA. Immunization of mice with H1 antigen along with different concentrations of PLG, ranging from 0.1 to 10 mg, led to a substantial increase in production of IgG isotype IgG1, IgG2a, and IgG2b antibodies ( $P < 0.05$  to  $0.01$ ,  $n = 5$ ) (Fig. 2B). The antibody response peaked at a dose of 1 mg of PLG, and no further increase was observed at higher concentration. At 1 mg PLG, both IgG1 and IgG2 titers were comparable to that of the control adjuvant CFA (Fig. 2B). A comparison of mouse groups adjuvanted with either PLG or alum demonstrated production of significantly higher levels of IgG2a antibodies ( $P < 0.01$ ), followed by IgG1 ( $P < 0.05$ ), in the PLG group, while IgG2b levels in the two groups were comparable. The above-described results indicated that PLG was able to augment the humoral response against an antigen in mice and resulted in significantly elevated levels of total IgG and its subclasses, viz., IgG1, IgG2a, and IgG2b, reflecting activation of both the Th1- and Th2-specific immune responses. Overall, the results demonstrated the adjuvant property of the isolated PLG peptides in a mouse model.

Further, to study the effect of PLG on Th cell development, memory recall response of the cultured splenocytes from differently immunized mouse groups was assessed by quantifying the cytokines released in the medium after stimulation with the antigen. From the above-described experiment the dose of 1 mg PLG per mouse seemed optimal, so further tests were performed at this dose only. In all mouse groups, stimulation of splenocytes by concanavalin A (ConA) led to secretion of different cytokines in the medium (data not shown). The mice immunized with adjuvants along with H1 antigen elicited a better cytokine response upon stimulation with the cognate



protein than the antigen-alone group (Fig. 2C). Immunization with CFA plus H1 showed the highest Th1-type cytokine response,  $1,036.3 \pm 175$  pg/ml of gamma interferon (IFN- $\gamma$ ) and  $699.3 \pm 136.1$  pg/ml of tumor necrosis factor alpha (TNF- $\alpha$ ), while alum was relatively less effective,  $268 \pm 177$  pg/ml of IFN- $\gamma$  and  $103.6 \pm 48.3$  pg/ml of TNF- $\alpha$  (Fig. 2C). In the PLG-adjuvanted group, the response was more in favor of Th1-type cytokines, IFN- $\gamma$  ( $844.3 \pm 297.4$  pg/ml) and TNF- $\alpha$  ( $556.3 \pm 188.2$  pg/ml), at levels  $\sim 14$ - and  $\sim 6$ -fold higher than that of the antigen-alone control mice ( $P < 0.01$  for both). Thus, the response of the PLG-immunized group was better than that of the alum group ( $P < 0.05$  for IFN- $\gamma$  and  $P < 0.01$  for TNF- $\alpha$ ) and comparable to that of the CFA-immunized groups (Fig. 2C). The interleukin-4 (IL-4) production in the PLG-adjuvanted mice was lower ( $197.3 \pm 72$  pg/ml) than those of both the CFA ( $488 \pm 64$  pg/ml) and the alum ( $324.3 \pm 85.4$  pg/ml) groups. Increased production of the isotypes IgG2a and IgG2b in the PLG-adjuvanted mice is consistent with elevated Th1-type IFN- $\gamma$  and TNF- $\alpha$  cytokines.

**Evaluation of adjuvant potential of PLG with different antigens.** Having established that 1 mg PLG as adjuvant was able to augment the immune response of H1 antigen, we proceeded to determine its ability to modulate the response of a panel of diverse, model antigens, viz., Ag85B, BP26, and protective antigen (PA) (Fig. 3A). Alum, a widely used adjuvant in human vaccines, was used for comparison. All three antigens by themselves were weakly immunogenic, as total IgG production was similar to that of the phosphate-buffered saline (PBS) control group. However, when the mice were immunized with the antigens along with PLG as the adjuvant, total IgG levels increased significantly in all three groups ( $P < 0.001$ ,  $P < 0.01$ , and  $P < 0.01$  for Ag85B, BP26, and PA, respectively) (Fig. 3B to D). To analyze the nature of the PLG-induced humoral response, generation of the antigen-specific, Th1-dependent IgG2a and IgG2b and Th2-dependent IgG1 isotypes was measured in the immune mouse serum. The PLG-adjuvanted mice produced significantly larger amounts of IgG1, IgG2a, and IgG2b isotypes in all three antigen groups than the respective antigen-alone controls (Fig. 3B to D). The increase in the titers due to PLG supplementation was highest in IgG2a ( $\sim 71$ -,  $\sim 41$ -, and  $\sim 39$ -fold), followed by IgG1 ( $\sim 39$ -,  $\sim 32$ -, and  $\sim 22$ -fold) and IgG2b ( $\sim 34$ -,  $\sim 28$ -, and  $\sim 17$ -fold) in the Ag85B-, BP26-, and PA-immunized mice, respectively. Alum and PLG as adjuvants were not significantly different in augmenting serum IgG1 titers against all three antigens (Fig. 3B to D). The alum-adjuvanted mice displayed a prominent Th2-biased immune response, indicated by heightened IgG1 titers in the Ag85B and PA groups ( $\sim 24$ - and  $\sim 19$ -fold;  $P < 0.01$ ) and in the BP26 group ( $\sim 23$ -fold;  $P < 0.05$ ) compared to antigen-alone groups. The Th1-specific response in the alum group was muted, recording relatively smaller increases in the titers of IgG2a ( $\sim 18$ -,  $\sim 13$ -, and  $\sim 18$ -fold) and IgG2b ( $\sim 15$ -,  $\sim 9$ -, and  $\sim 6$ -fold) against Ag85B, BP26, and PA, respectively. In contrast, the Th1-specific response of PLG-adjuvanted antigens showed significantly higher values of both IgG2a and IgG2b titers than alum-adjuvanted groups ( $P < 0.05$ ) (Fig. 3B to D). Further, augmentation of both Th1- and Th2-dependent antibody titers against diverse antigens showed PLG as a broad-acting adjuvant. Altogether, supplementation of the three control antigens with PLG led to

**FIG 2** Effect of PLG adjuvantation on immune response of H1 (Ag85B-ESAT-6) antigen. (A) C57BL/6J mice were immunized by the i.p. route with 20  $\mu$ g of fusion antigen H1 alone or with different concentrations (0.1, 0.5, 1, and 10 mg) of PLG or with control adjuvants CFA (1:1 with antigen) and alum (200  $\mu$ g) in a total volume of 0.2 ml. Antigen H1-specific total IgG and isotypes were evaluated in the sera of individual mice ( $n = 5$ ) by ELISA 3 weeks after immunization. (B) Antibody titers of total IgG and isotypes IgG1, IgG2a, and IgG2b. (C) Three weeks after immunization, splenocytes were isolated and cultured *in vitro* with H1 antigen for 72 h, and release of IFN- $\gamma$ , TNF- $\alpha$ , and IL-4 was measured in the culture supernatant by ELISA. Each point represents means of triplicate values from individual mice, and the bars represent mean values from all mice in a group, with standard errors of the means (SEM). In antibody titer studies, for comparing the data obtained from the antigen-alone group with an adjuvanted group, between two different adjuvanted groups, or between two different doses of the same adjuvanted group, the  $P$  value was calculated by unpaired  $t$  test. One-way ANOVA followed by Tukey's multiple-comparison test was used for cytokine analysis. The limits of the bars on top extend between test samples compared for statistical significance. \*,  $P < 0.05$ ; \*\*,  $P < 0.01$ ; \*\*\*,  $P < 0.001$ . n.s., nonsignificant.

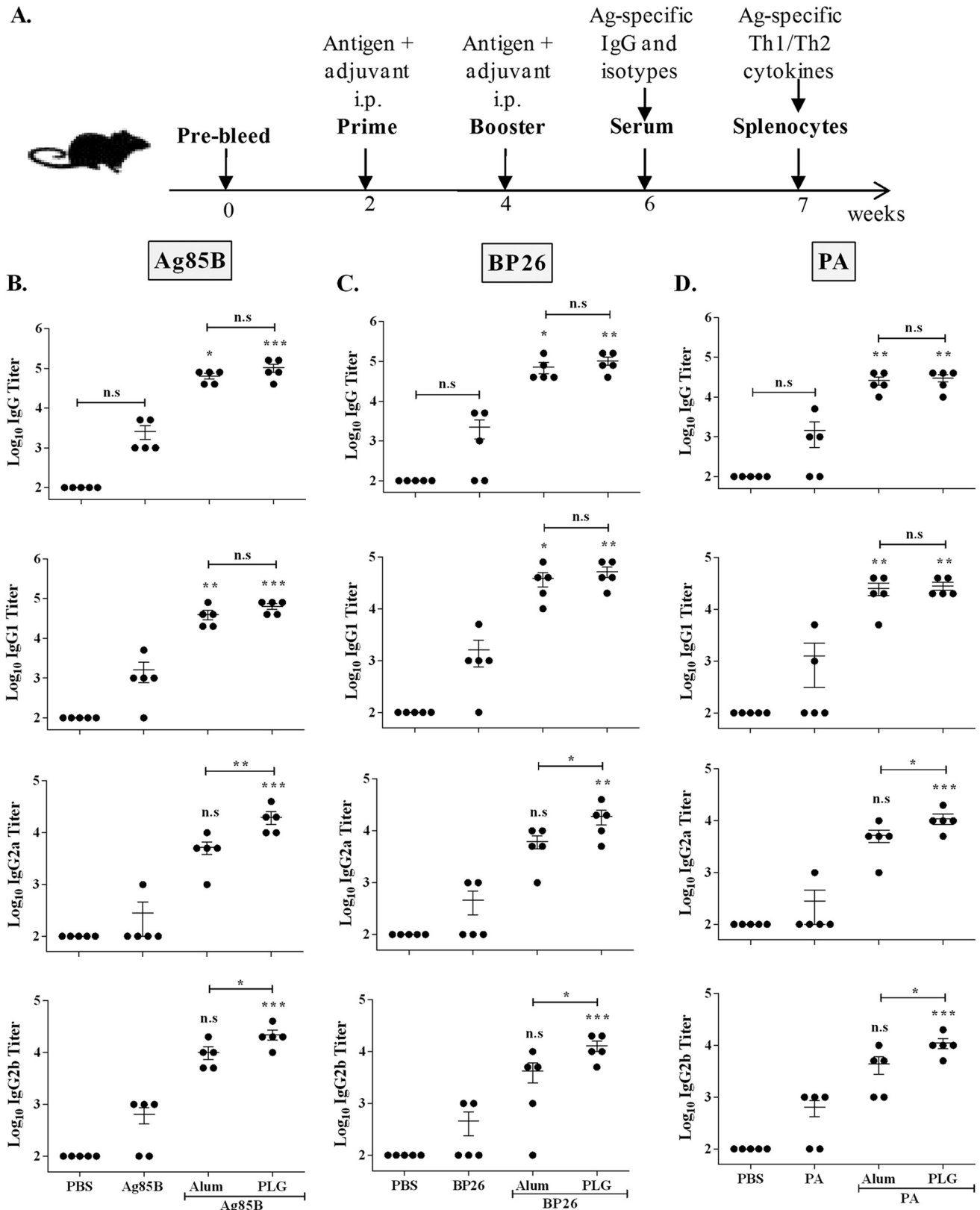


**FIG 3** Modulation of humoral immune response of different antigens by PLG adjuvantation. (A) Mice were immunized intraperitoneally with individual antigens (20  $\mu$ g of Ag85B, BP26, or PA) or with PLG (1 mg) or alum (200  $\mu$ g) in a volume of 0.2 ml, and antigen-specific antibodies in the sera were measured by ELISA 2 weeks after the final immunization. (B to D) Antigen Ag85B (B)-, BP26 (C)-, and PA (D)-specific total IgG and subtype (IgG1, IgG2a, and IgG2b) titers were measured in individual mice ( $n = 5$ ). One-way ANOVA followed by Tukey's multiple-comparison test was employed for calculating the significant difference. \*,  $P < 0.05$ ; \*\*,  $P < 0.01$ ; \*\*\*,  $P < 0.001$ . n.s., nonsignificant.

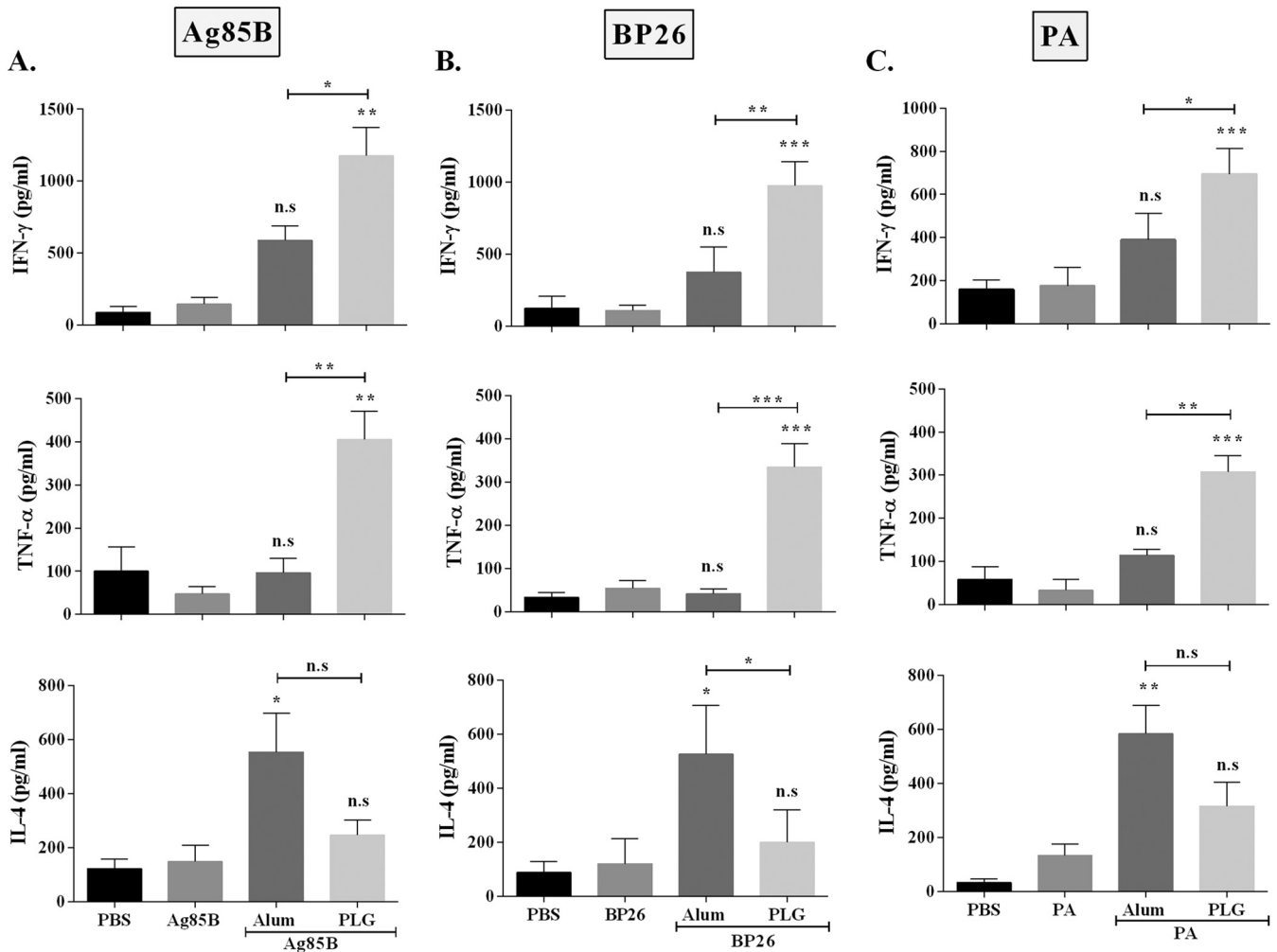


**FIG 4** Modulation of cytokine response of different antigens by adjuvantation with PLG. Three weeks after the last immunization, splenocytes were isolated and cultured *in vitro* with the respective antigens for 72 h, and release of antigen-specific cytokines was measured in the culture supernatant by ELISA. (A to C) Antigen Ag85B (A)-, BP26 (B)-, and PA (C)-specific cytokines IFN- $\gamma$ , TNF- $\alpha$ , and IL-4 were measured in individual mice ( $n = 3$ ). One-way ANOVA followed by Tukey's multiple-comparison test was employed for calculating the significant difference. \*,  $P < 0.05$ ; \*\*,  $P < 0.01$ ; \*\*\*,  $P < 0.001$ . n.s., nonsignificant.

enhancement of antigen-specific serum IgG and its isotypes (IgG1, IgG2a, and IgG2b), demonstrating a Th1-dominant immune response orchestrated by the adjuvant.

To examine the corresponding effect of PLG on the cytokine response, splenocytes from the mouse groups immunized with the three antigens either alone or with adjuvants were stimulated with the respective antigen, and the memory recall response was assessed by quantifying the Th1-specific (TNF- $\alpha$  and IFN- $\gamma$ ) and Th2-specific (IL-4) cytokine levels in the culture supernatant. Splenocytes from the mice immunized with Ag85B, BP26, or PA alone produced low levels of the three cytokines, IFN- $\gamma$  ( $144 \pm 78$ ,  $107 \pm 37$ , and  $176 \pm 84$  pg/ml), TNF- $\alpha$  ( $47 \pm 31$ ,  $54 \pm 30$ , and  $133 \pm 71$  pg/ml), and IL-4 ( $148 \pm 106$ ,  $120 \pm 92$ , and  $33 \pm 45$  pg/ml), which were similar to those of the PBS controls (Fig. 4A to C). When the antigens were supplemented with PLG as the adjuvant, the splenocytes produced significantly larger amounts of IFN- $\gamma$  ( $1,176 \pm 343$ ,  $976 \pm 166$ , and  $694 \pm 123$  pg/ml) and TNF- $\alpha$  ( $405 \pm 113$ ,  $335 \pm 95$ , and  $307 \pm 65$  pg/ml) against all three antigens, Ag85B, BP26, and PA, respectively. However, the levels of Th2-specific IL-4 in the PLG-adjuvanted group were relatively lower ( $246 \pm 98$ ,  $200 \pm 121$ , and  $317 \pm 151$  pg/ml) than when alum was used as the adjuvant ( $555 \pm 250$ ,  $526 \pm 180$ , and  $585 \pm 183$  pg/ml) in all three antigens, Ag85B, BP26, and PA, respectively (Fig. 4A to C). The increased production of Th1-specific IFN- $\gamma$  and TNF- $\alpha$  cytokines in the PLG-adjuvanted group reiterates the immunomodulatory capability of



PLG in the mouse model. The results demonstrate that the PLG peptides function as an adjuvant to enhance the immune response of antigens of diverse bacterial origin.

**Evaluation of PLG as adjuvant in modulating immune response and protective efficacy of ESAT-6 antigen against *M. tuberculosis* infection in mice.** The above-described results showed that addition of PLG to different proteins significantly augmented antigen-specific Th1-type responses known to be important in providing protective immunity against intracellular pathogens like *Salmonella enterica* serovar Typhi and *M. tuberculosis*, etc. (10, 11). Thus, we proceeded to evaluate the ability of PLG in enhancing protective efficacy of ESAT-6, used as a vaccine candidate against *M. tuberculosis* H37Rv infection in mice. The parameters of protective immunity, such as humoral response, recall memory to the antigen, clearance/reduction in bacterial load, and long-term survival of the host, etc., were examined after *M. tuberculosis* infection in PLG-adjuvanted mice (Fig. 5A). For comparison we used dimethyl-dioctadecyl ammonium bromide-monophosphoryl lipid A (DDA-MPL), a well-known Th1 immunity-inducing adjuvant, and BCG (TUBERVAC, Serum Institute of India), the only approved vaccine against tuberculosis.

Two weeks after the final immunization, ESAT-6, with low immunogenicity, failed to mount a significant antibody response, as expected (Fig. 5B). In contrast, both the PLG- and DDA-MPL-adjuvanted mice showed significant increases in the production of total IgG and its isotypes, with IgG2a being the predominant one, followed by IgG2b and IgG1. Compared to ESAT-6 alone, the PLG-adjuvanted mice displayed ~25-, ~68-, and ~30-fold and the DDA-MPL group ~21-, ~35-, and ~25-fold increases in IgG1, IgG2a, and IgG2b titers, respectively (Fig. 5B). Notably, IgG2a titers were significantly higher in the PLG-immunized mice than in the DDA-MPL group ( $P < 0.05$ ) (Fig. 5B). Consistent with earlier results, it is concluded that PLG modulated the immune response of ESAT-6-immunized mice by stimulating production of the Th1- and Th2-dependent IgG2a, IgG2b, and IgG1 antibodies in a balanced manner.

The splenocytes from vaccinated mice were tested for recall memory after antigenic stimulation by quantifying the Th1-dependent (TNF- $\alpha$ , IFN- $\gamma$ , and IL-2), Th2-dependent (IL-4, IL-6, and IL-10), and Th17-dependent (IL-17A) cytokines, released in the medium after 72 h of incubation. The amounts of all cytokines produced by ESAT-6-immunized mice were quite low and similar to that of the PBS control (Fig. 5C). On supplementing ESAT-6 with PLG, the levels of cytokines IFN- $\gamma$  ( $6,072 \pm 1,026$  pg/ml), TNF- $\alpha$  ( $2,200 \pm 696$  pg/ml), IL-2 ( $621 \pm 276$  pg/ml), IL-6 ( $2,296 \pm 413$  pg/ml), and IL-10 ( $2,623 \pm 1,695$  pg/ml) increased significantly in the medium (Fig. 5C). Although DDA-MPL also enhanced ESAT-6-specific responses of the splenocytes, producing IFN- $\gamma$  ( $3,742 \pm 1,986$  pg/ml), TNF- $\alpha$  ( $945 \pm 204$  pg/ml), IL-2 ( $455 \pm 255$  pg/ml), IL-6 ( $1,376 \pm 312$  pg/ml), and IL-10 ( $3,207 \pm 715$  pg/ml) cytokines, the increase in Th1-dependent cytokine levels was more pronounced in the ESAT-6-plus-PLG-vaccinated mice. IL-10 secretion also increased in both PLG and DDA-MPL groups after stimulation with ESAT-6 compared to antigen alone; however, the increase was significant only in the DDA-MPL group ( $P < 0.05$ ) (Fig. 5C). In contrast to the robust IFN- $\gamma$  or IL-6 responses observed with PLG or DDA-MPL supplementation, the increase in IL-4 level was relatively low (18 pg/ml for PLG and 20 pg/ml for DDA-MPL), as noted in the earlier experiments as well. More importantly, after stimulation with ESAT-6, significantly higher levels of IL-17A ( $7,490 \pm 508$  pg/ml) were produced solely in the PLG-supplemented group and not with DDA-MPL or antigen-alone groups ( $P < 0.0001$ ) (Fig. 5C). Thus, considering its consistent positive immunomodulatory action on the Th1-, Th2-, and also Th17-type IL-17A effectors, PLG appears to be a promising adjuvant candidate.

Since the above-described results established that PLG modulated the immune response of the mycobacterial antigen ESAT-6 in mice, its effect on protective efficacy was also evaluated. Six weeks after the final immunization, the remaining vaccinated mice were challenged with the virulent *M. tuberculosis* strain H37Rv through the intravenous (i.v.) route. At each time point, four mice from each group were sacrificed, and CFU counts in the lung and spleen were determined. Six weeks after infection, ESAT-6 alone reduced the bacterial load marginally in the lungs and spleens of mice

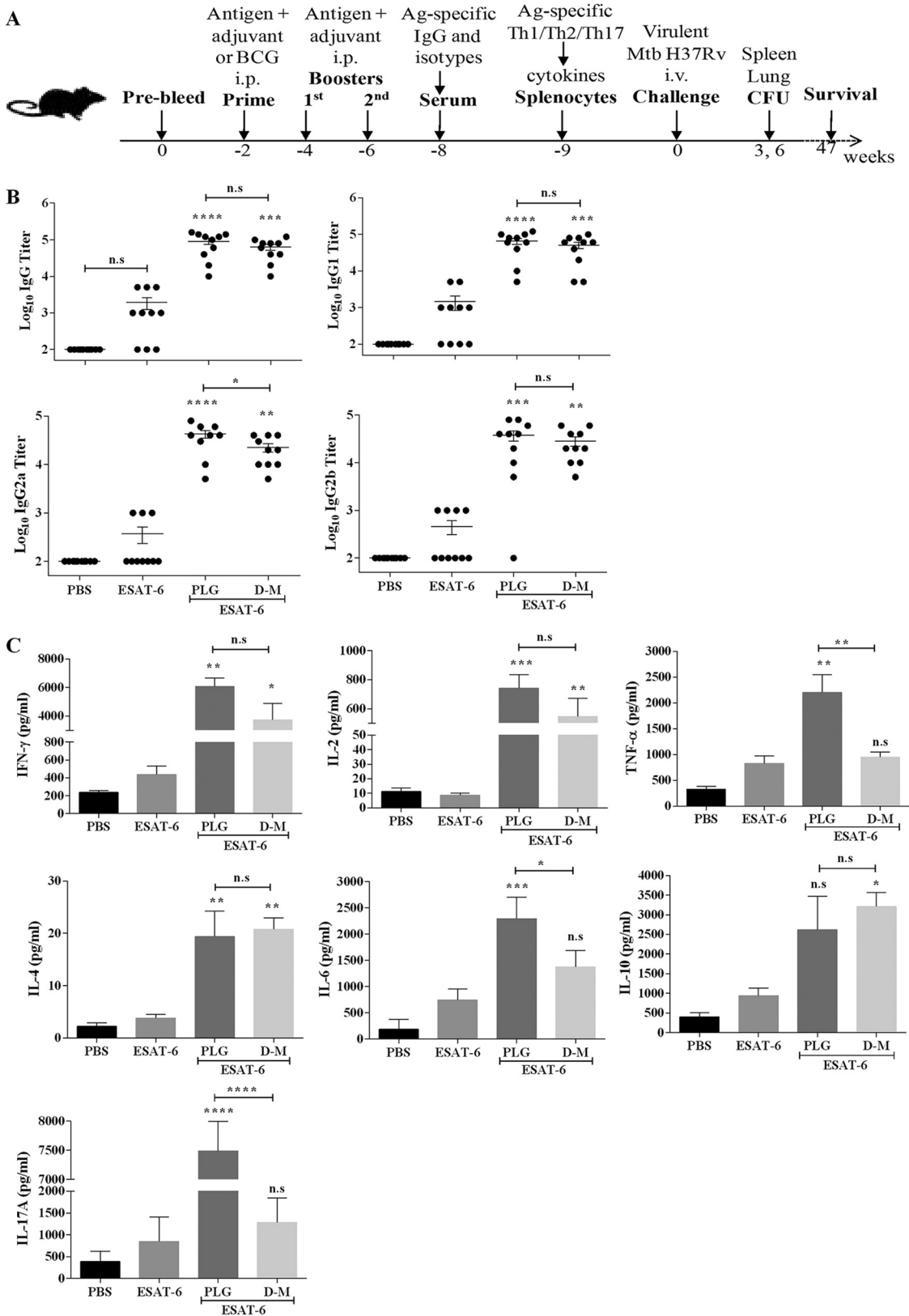


**FIG 5** Modulation of immune response against antigen ESAT-6 by PLG adjuvantation. (A) C57BL/6J mice were immunized intraperitoneally with 20  $\mu$ g of antigen ESAT-6 either alone or in the presence of PLG (1 mg) or control adjuvant DDA-MPL (250:25  $\mu$ g). Antigen ESAT-6-specific total IgG and isotypes were measured in the serum samples of individual mice ( $n = 10$ ) by ELISA. (B) Titers of total IgG and its isotypes, IgG1, IgG2a, and IgG2b, 2 weeks after the final immunization. (C) Three weeks after the last immunization, splenocytes were isolated and cultured *in vitro* with antigen ESAT-6 for 72 h, and release of IFN- $\gamma$ , IL-2, TNF- $\alpha$ , IL-4, IL-6, IL-10, and

(Continued on next page)

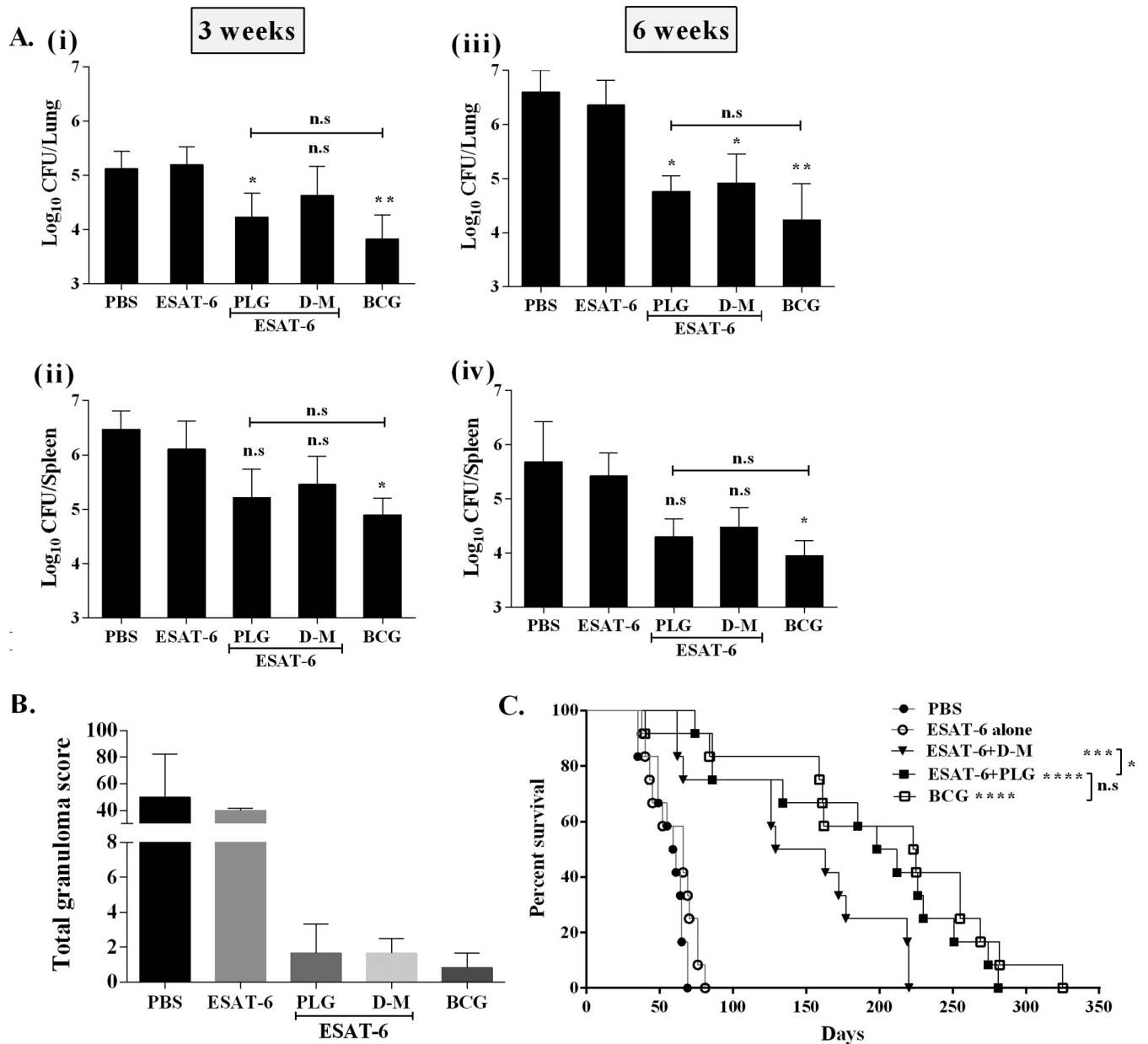


**FIG 6** Evaluation of protective efficacy of ESAT-6 by adjuvination with PLG against *M. tuberculosis* infection. The mice were immunized by the i.p. route with antigen ESAT-6 either alone or with adjuvants. BCG vaccine was given at the time of the first immunization. Six weeks after the last immunization, the mice were challenged with a virulent strain of *M. tuberculosis* H37Rv by the i.v. route. (A) Four mice from each group were sacrificed at each time point after challenge, and the CFU in the lung and spleen were recorded. (i and ii) Lung (i) and spleen (ii) *M. tuberculosis* load at 3 weeks. (iii and iv) Lung (iii) and spleen (iv) *M. tuberculosis* load at 6 weeks. (B) Graphical representation of total granuloma score from each infected mouse group. (C) Survival of *M. tuberculosis*-infected mice ( $n = 12$ ) from each group, monitored for death until 47 weeks. The results are presented as percent survival. One-way ANOVA followed by Tukey's multiple-comparison test was employed for calculating the statistical significance in CFU studies. To calculate the significance of difference in survival studies, the log-rank Mantel-Cox tests were applied. \*,  $P < 0.05$ ; \*\*,  $P < 0.01$ ; \*\*\*,  $P < 0.001$ ; \*\*\*\*,  $P < 0.0001$ . n.s, nonsignificant.

compared to the nonvaccinated (PBS) group (Fig. 6A), while the highest reduction was observed in BCG-vaccinated mice ( $P < 0.01$  for lung and  $P < 0.05$  for spleen). Both PLG- and DDA-MPL-adjuvanted mice also showed reduction in the bacillary load of lung 6 weeks postchallenge compared to mice immunized with antigen alone ( $P < 0.05$ ). In

**FIG 5** Legend (Continued)

IL-17A was measured in the culture supernatant. The mouse group D-M indicates the adjuvant DDA-MPL. One-way ANOVA followed by Tukey's multiple-comparison test was employed for calculating the significant difference. \*,  $P < 0.05$ ; \*\*,  $P < 0.01$ ; \*\*\*,  $P < 0.001$ ; \*\*\*\*,  $P < 0.0001$ . n.s, nonsignificant.

the ESAT-6-plus-PLG-immunized group, reduction of  $1.599 \log_{10}$  CFU in the lungs and  $1.121 \log_{10}$  CFU in the spleen was observed (Fig. 6A). Although the BCG-immunized mice showed the highest reduction in bacillary counts in the lung and spleen ( $2.323$  and  $1.469 \log_{10}$  CFU, respectively), statistically the result was not different from that of ESAT-6-plus-PLG-adjuvanted mice, reaffirming the role of PLG as an effective adjuvant.

Histopathology of the lungs revealed higher numbers of granulomatous lesions in the nonvaccinated (PBS) and ESAT-6-vaccinated mice, with mean granuloma scores of 50 and 40, respectively (Fig. 6B). Both the DDA-MPL- and PLG-adjuvanted mice displayed much lower granuloma scores (1.66) than the antigen-alone and placebo mouse groups. The BCG-vaccinated mice showed even fewer granulomatous lesions (granuloma score, 0.83), similar to healthy, uninfected mice (Fig. 6B). Further, the PLG- or DDA-MPL-adjuvanted mice showed smaller alveolar spaces, possibly due to a lower degree of inflammation (data not shown).

In addition to assessing the bacterial burden and histopathology, we monitored long-term survival of the mice after *M. tuberculosis* challenge. The degree of protection was evaluated by monitoring different parameters of infection (general appearance, difficulty in breathing, weight loss, and death) until 47 weeks. The PBS-immunized control group showed significant weight loss ( $4.46 \pm 1.54$  g) and fur loss 6 weeks after infection and died early, with a median survival time (MST) of 60 days (Fig. 6C). Similarly, all mice immunized with ESAT-6 alone died of infection, with a marginal increase in MST to 66 days. The MST was prolonged to 146 days in the mice immunized with DDA-MPL plus ESAT-6. In the ESAT-6-plus-PLG-immunized group, the mice were active and healthy, with mean weight gain of  $2.7 \pm 0.93$  g (6 weeks postchallenge) and prolonged MST of 205 days. Thus, PLG as an adjuvant appears to be better than DDA-MPL in enhancing the protective efficacy of ESAT-6. The degree of protection was highest in the BCG-vaccinated mice, reflected by longer MST (224 days) ( $P < 0.0001$ ), which matched well with maximum reduction in the bacterial load as well (Fig. 6C). Notably, the overall degree of protection in the BCG-vaccinated group was statistically not different from that of the PLG-adjuvanted group. Thus, to sum up, the above-described results support the conclusion that PLG as an adjuvant can enhance protective efficacy of an antigen by activating specific components of the immune system in mice.

## DISCUSSION

Our research is focused on deciphering the biological significance of a high-molecular-weight polymer, PLG, in the cell wall of pathogenic mycobacteria (35). PLG biosynthesis is linked to a functional extracellular glutamine synthetase (eGS), an important virulence determinant necessary for growth and survival of *M. tuberculosis* in the host (33). In light of the association of PLG with the eGS, we were motivated to investigate its biological properties in more detail. The *M. tuberculosis* cell wall components are known to be highly immunostimulatory in nature and are formulated as mannide mono-oleate emulsions in CFA. However, due to toxicity of the formulation, application of CFA as the adjuvant is restricted to animal models only (24). Taking a cue from the reported immunomodulatory properties of different biomolecules of the *M. tuberculosis* cell wall (11, 25, 26), we isolated PLG from the cell envelope and explored its suitability as an adjuvant in mice using a variety of model antigens.

Ours is the first comprehensive report dealing with the adjuvant potential of PLG in modulating host immune responses to an array of prototypical antigens, like ESAT-6, Ag85B, PA, and BP26. Stimulation of the immune response by PLG led to manifestation of antigen-specific Th1-dependent IgG2a and IgG2b and Th2-specific IgG1 antibodies, indicating effective presentation of the antigen with major histocompatibility complex class II molecules and subsequent activation of both Th1 and Th2 arms of immunity. The higher IgG production and isotype switching predominantly to IgG2a by PLG adjuvantation is consistent with enhanced production of the Th1-dependent IFN- $\gamma$  and TNF- $\alpha$  cytokines. Moreover, minimal immunogenicity of PLG precluded the risk of its masking the antigen response and reaffirmed its suitability as an adjuvant candidate. Considering the essential role of an adjuvant in defining the quality of immune

response, activation of Th1 response, a necessary component of protective immunity against infectious diseases (36), is an important attribute of the glutamine polymer. A small, chemically defined glutamine-rich peptide (Q11), conjugated to self-assembling peptide epitopes, was shown to act as an adjuvant in mice; the Q11 peptides, although providing help in generating a strong antibody response, were not able to evoke cell-mediated immunity (28), as observed in our study. It is difficult to assign a reason for this discrepancy. A possible explanation, subject to experimental verification, is a shorter length and nonnative molecular structure/organization of the glutamine polypeptide. Thus, it appears that upregulation of the Th1-specific effectors IFN- $\gamma$ , TNF- $\alpha$ , and IL-2 and Th2-specific IL-6 and IL-10 cytokines, in cooperation with the elevated levels of antibodies, helped in generating a robust memory response in the PLG-adjuvanted mice.

The adjuvants modulating host response toward Th1 cell-dependent immunity are in high demand, as they play a key role in attaining long-lasting immune memory and effective protection against intracellular pathogens, like *M. tuberculosis*, *Salmonella enterica* serovar Typhi, etc. (12, 13). The well-known aluminum salts or the squalene-based adjuvants like AS03 and MF59, licensed for human use, are known to be poor inducers of Th1 immunity (10, 36, 37). Other adjuvants, like CAF01, IC31, GLA-SE, and CpG ODN, etc., that induce significant levels of the Th1-specific cytokines during TB infection are still in different stages of clinical testing (20, 38–40). Hence, in the present scenario the ability of PLG to induce a broad-based, multifaceted immune response to antigens from different sources (Ag85B, ESAT-6, PA, and BP26) on par with CFA and better than alum and DDA-MPL is highly desirable and demands further promotion.

The efficacy of a vaccine is judged mainly by the degree of protection it provides to the recipient host. The ability of PLG to modulate protective efficacy of the vaccine candidate ESAT-6 can be observed at different levels of host response. The activation of Th1- and Th2-specific cytokines to the generation of a repertoire of antibodies and the reduction of the bacterial burden in the lungs and spleen work together to generate a robust host response. A significant outcome of PLG adjuvantation is reflected by extension of the mean survival time of mice equivalent to the level of BCG vaccination. The activation of Th17 cells with a subsequent increase in the secretion of IL-17A is another distinctive property of PLG that might have played a role in improving the protective efficacy of ESAT-6 (Fig. 6C). Recently, the Th17 cells have emerged as key players in protection against TB by triggering a series of events, beginning with chemokine synthesis to promotion of T and B cell localization and activation of the *M. tuberculosis*-infected macrophages in the lung granulomas, which together contain the spread of *M. tuberculosis* to other organs (41). Vaccines containing H1 and H28 fusion antigens of *M. tuberculosis* with CAF01 were shown to elicit long-lasting Th17 responses, imparting sustained protection against TB (42). Thus, in light of the above-described results, it is concluded that PLG adjuvantation is responsible for manifestation of a robust immune response against ESAT-6, enhancing protective efficacy of the latter against *M. tuberculosis* challenge.

The exact underlying mechanism of the adjuvant activity of PLG is not clear at this stage. Immunomodulatory activity of bacterial products is attributed to their similarity to microbial ultrastructures, referred to as pathogen-associated molecular patterns (PAMPs), which are perceived as a danger signal of infection by the host (43). Indeed, pattern recognition receptors (PRRs), such as Toll-like receptors (TLRs), on the cell surface of the APCs are believed to interact with an antigen through the PAMPs and activate downstream signaling pathways that trigger the adaptive immune response (43). It is possible that inclusion of additional PAMPs as PLG adjuvant has broadened the immune recognition process of the host, improving efficacy of the vaccine. Alternatively, PLG might have acted as a carrier for antigens by either entrapment or noncovalent binding, facilitating endosomal entry into the APCs to produce improved antigen-specific immune responses. Indeed, the ultrastructure of purified PLG showed large aggregates containing long chains of globules, with an average size of  $\sim 23.14$  nm (Fig. 1C), which might have provided scaffolding for better adsorption of the antigen. Additionally, due to its particulate nature, PLG may slow down

or resist proteolytic cleavage in the eukaryotic proteasome (44) and exert a “depot effect” by increasing residence time at the site of vaccination, thereby promoting activation of the APCs and phagocytosis. A similar mechanism of action has been reported for synthetic poly(lactic-co-glycolic acid) (PLGA) particles (45), virus-like particle (VLP)-based vaccines (46, 47), and the immune-stimulating complexes (ISCOMS) (48). Presently, sustained efforts are needed to reduce the dosage of PLG for optimum action. A better understanding of the mechanism of action of PLG would help design chemically defined, pathogen-specific combinatorial formulations for mechanistic orchestration of the host immune response.

It has to be mentioned here that, with this being the first attempt to study the adjuvant potential of PLG, the scope of examination had to be limited to basic essential parameters. To obtain detailed information about immunological properties of PLG, a multitude of factors, like immunization protocol, antigen concentration, adjuvant dose, immunization route, and window of time before infection/challenge, etc., likely to influence the outcome, could not be included in a single study. In the course of development of a novel immunomodulator projected for future human use, factors such as the route of immunization and dosage of the antigen/adjuvant are critical and require comprehensive optimization protocols. Studies are in progress in our laboratory to achieve these objectives. In the present study, we chose the intraperitoneal (i.p.) route, as it is frequently used and was found to be more effective for rodents (49–51). Schmidt et al. have shown that administration of CAF09 adjuvant via the intramuscular or subcutaneous route elicited weaker CD8<sup>+</sup> T-cell responses than the i.p. route (52). Moreover, challenge of mice with *M. tuberculosis* has been performed via both the intravenous (high-dose) and the respiratory aerosol (low-dose) route (22, 53). The latter, being closer to the physiological route, would have been ideal for *M. tuberculosis* infection; however, due to experimental and technical limitations, this could not be performed at this stage. Hence, we opted for the intravenous, high-dose ( $2.3 \times 10^5$  CFU) challenge model in the present study. Further, we have not investigated the mechanistic aspect of immunomodulation by PLG, which is necessary for expanding the range of applications of PLG as an adjuvant. Nonetheless, owing to the consistent immunostimulating profiles of PLG across different antigens, we were encouraged to report this study describing PLG as an efficient Th1-type adjuvant.

In conclusion, our study has revealed that the naturally occurring PLG peptides of *M. tuberculosis* origin act like an archetypical adjuvant that modulates both the humoral and cell-mediated arm of host immunity. An adjuvant plays a key role in the successful deployment of a vaccine; the fact that the purified PLG produced no apparent adverse effect in mice and in the THP-1 macrophage culture (data not shown) advocates for its suitability as a biological material for testing in animal models. To broaden the scope of PLG as an adjuvant, it would be worthwhile to explore its potential in vaccines against other intracellular pathogens. To promote its acceptance as an adjuvant, PLG needs to be subjected to a higher level of scrutiny on immunologic and toxicological parameters. Our study has performed the groundwork and provides data demonstrating that PLG is a promising vaccine delivery vehicle, particularly for chronic infectious diseases.

## MATERIALS AND METHODS

**Bacterial strains, plasmids, and culture conditions.** All of the recombinant plasmids and bacterial strains used in this study are indexed in Table S1 in the supplemental material. For protein expression and purification, all of the *Escherichia coli* recombinant strains were cultured in Luria-Bertani (LB) medium (Difco) under standard conditions. *M. tuberculosis* cultures were grown as described earlier by Gupta et al. (54). All of the cultures were grown at 37°C with shaking at 180 rpm.

**Isolation of PLG peptides from *M. tuberculosis* H37Rv.** The PLG polypeptides were extracted from the *M. tuberculosis* cell wall fractions, as described earlier by Hirschfield et al. (29), with multiple modifications. Briefly, *M. tuberculosis* H37Rv cells were grown until stationary phase (optical density at 600 nm [OD<sub>600</sub>] of ~1.6), harvested, and heat killed at 90°C for 2 h, followed by washing twice with distilled water for cell wall preparation (29). The cell walls were treated with 0.1% trypsin-chymotrypsin (1:1, wt/vol) at room temperature overnight, followed by delipidation, once with acetone, twice with chloroform-methanol (2:1), and twice with diethyl-ether. The pellet was air dried to remove residual amounts of the organic solvents (31) and subjected to 2% (wt/vol) SDS extraction at 60°C in a water bath for 2 h to eliminate the membrane components and soluble proteins. The insoluble fraction was recovered by centrifugation at 20,000 rpm and then sequentially washed with PBS, distilled water, and

80% (vol/vol) aqueous acetone to exclude traces of SDS. The resulting product, mainly containing SDS-insoluble constituents of the cell wall, including PLG peptides, was subjected to density gradient centrifugation, first in discontinuous sucrose and second in 80% Percoll solution (GE Healthcare), as described earlier by Hirschfield et al. (29).

**Chemical and physical analysis of PLG.** The chemical nature of the *M. tuberculosis* cell wall-isolated PLG peptides was examined by gas chromatography-mass spectrometric (GC-MS) analysis as described earlier by Garg et al. (35). NIST 05 and WILEY8 chemical libraries were used to analyze the GC-MS data. Total carbohydrate, protein, lipid, and nucleic acid contamination was estimated as described earlier (55–58).

The PLG peptides were resolved by high-resolution Tricine-based SDS-PAGE (59) using 0.2 M Tris-HCl (pH 8.9) as anode buffer and 0.1 M Tris-HCl, 0.1 M Tricine, and 0.1% SDS (pH 8.25) as cathode buffer. Electrophoresis was initially carried out at 40 V for 1 h, followed by 100 V for the next 2 h, at room temperature. Protein was visualized by Coomassie blue staining. For immunoblotting, the peptides were transferred to a nitrocellulose membrane using Tris-glycine transfer buffer (25 mM Tris-HCl and 200 mM glycine) for 1 h at 4°C. The membrane was incubated with 3% bovine serum albumin in PBS-T (0.1% Tween 20 in PBS) for 1 h at room temperature, washed with PBS-T, and probed with anti-polyglutamine monoclonal antibodies produced in mouse (1:500) (P1874-200UL; Sigma-Aldrich) for 1 h at room temperature. The membrane was washed with PBS-T thrice and incubated with anti-mouse alkaline phosphatase (AP)-conjugated secondary antibodies (1:5,000) for 1 h at room temperature. After washing with PBS-T, the blot was developed with an AP conjugate substrate kit (1706432; Bio-Rad) for detection.

Morphological characterization of *M. tuberculosis* PLG at the ultrastructural level was achieved by transmission electron microscopy (TEM). Briefly, 1 mg of purified PLG sample in 100  $\mu$ l PBS was applied on carbon-coated copper grids and air dried for 5 min. The grids were negatively stained with 50  $\mu$ l of 2%, wt/vol, uranyl acetate for 5 min and viewed in an electron microscope (Jeol-JEM 2100F) with accelerating voltage of 80 to 200 kV.

The solubility profile of PLG was determined in various organic and inorganic solvents. Briefly, 5 mg of PLG was added to 1 ml of the solvent at room temperature with continuous stirring for 30 min. The amount of insoluble material obtained at the end was collected by centrifugation, dried, and weighed, and percent solubility was calculated.

**Protein expression and purification.** The recombinant antigens used in this study, viz., Ag85B and ESAT-6 of *M. tuberculosis* and PA of *Bacillus anthracis* (60), were expressed in *E. coli*. Briefly, the coding regions of all the antigens were PCR amplified using genomic DNA of the respective host and gene-specific forward and reverse primers. For constructing the recombinant fusion antigen Ag85B-ESAT-6, the *fbpB* (Ag85B) and *esxA* (ESAT-6) genes were fused at a unique KpnI site, using specific primers. All of the amplified DNA sequences were cloned under the isopropyl- $\beta$ -D-thiogalactopyranoside (IPTG)-inducible T5 promoter of pQE30 vector and expressed in *E. coli* M15 cells (Qiagen) at 37°C for 4 h. The His<sub>6</sub>-tagged recombinant proteins were purified under denaturing conditions with urea, followed by refolding on a nickel-nitrilotriacetic acid (Ni-NTA) affinity column (Qiagen), as described previously by Singh et al. (61). The BP26 antigen of *Brucella abortus* was cloned and expressed in *E. coli* BL21 cells using the pET28a expression system (Novagen) as described above. All of the protein fractions were dialyzed against 50 mM Tris-HCl buffer (pH 8.0) containing 0.3 M NaCl and 10% glycerol and stored at –80°C until further use. The identity of the recombinant proteins was confirmed by peptide mass fingerprinting. The antigens used in this study were examined by SDS-PAGE and immunoblot analysis using antisera raised against recombinant proteins. For details, see Fig. S1 in the supplemental material.

**Animals.** For immunization, 4- to 6-week-old, inbred, female C57BL/6J mice were used in the study. The mice were purchased from the National Centre for Laboratory Animal Sciences (NCLAS), Hyderabad, India. They were housed within microisolator cages at biosafety level 3, maintained under pathogen-free conditions, and fed pelleted food and water *ad libitum*. The study was approved by the Institutional Animal Ethics Committee (IAEC) and Biosafety Committee (IBSC) of Jawaharlal Nehru University, New Delhi, India.

**Mouse immunization and challenge.** For dose optimization, mice were immunized either with the fusion antigen Ag85B-ESAT-6 alone (20  $\mu$ g per dose) or with various concentrations of PLG (0.1, 0.5, 1, and 10 mg per mouse) by the intraperitoneal (i.p.) route. Each group ( $n = 5$ ) was given a single dose of the vaccine formulation. Some well-characterized commercial adjuvants, like alum (100  $\mu$ g per dose) (Sigma-Aldrich) and Freund's complete adjuvant (CFA; Sigma-Aldrich), mixed 1:1 with antigen in PBS in a dose of 0.2 ml per mouse, were used for comparison.

The adjuvant potential of PLG peptides was evaluated with a panel of protein antigens, viz., Ag85B, BP26, and PA. Each group of mice ( $n = 10$ ) was immunized by the i.p. route with vaccines containing either the individual antigens alone (20  $\mu$ g each) or adjuvant PLG (1 mg) in a 0.2-ml total volume, and for comparison, alum (200  $\mu$ g/mouse) was also included in the test. Two weeks after the first immunization, a single booster injection was given to the mice.

To evaluate the effect of PLG on protective efficacy of ESAT-6 vaccine, groups of mice ( $n = 24$ ) were immunized thrice at 2-week intervals between each immunization. The vaccines contained antigen ESAT-6 alone (20  $\mu$ g/mouse) or adjuvanted with 1 mg PLG in a total volume of 0.2 ml per mouse. DDA-MPL, mixed at a ratio of 250:25  $\mu$ g/mouse, was used as a control. Three weeks after the final immunization, 4 mice from each group were sacrificed for splenocyte culturing. As a positive control of protection, a group of mice was vaccinated with a single dose of BCG ( $1 \times 10^6$  cells/mice) at the time of first immunization. Six weeks after the last immunization, the remaining vaccinated mice (20 mice/group) were challenged by injecting  $\sim 2.3 \times 10^5$  *M. tuberculosis* H37Rv CFU/mouse by the i.v. (lateral tail vein) route, and subsequently four mice from each group were sacrificed at regular intervals

of 3 and 6 weeks for analysis. The remaining vaccinated and *M. tuberculosis*-challenged mice from each group ( $n = 12/\text{group}$ ) were monitored for weight loss, behavioral changes, and survival/death due to infection for the next 47 weeks.

**Measurement of antigen-specific antibodies in serum.** For dose optimization studies, blood was collected 3 weeks after the immunization by retro-orbital bleeding ( $n = 5$ ) and sera were prepared. For adjuvant potential and protective efficacy studies, sera were collected from 5 and 10 mice, respectively, 2 weeks after the final immunization. The antigen-specific antibody titers of IgG and its isotypes, namely, IgG1, IgG2a, and IgG2b, were measured by indirect enzyme-linked immunosorbent assay (ELISA) as described previously (25), with minor modifications. Briefly, high-binding 96-well microtiter plates (NuncMaxiSorp) were precoated with the capture antigen (500 ng/well) in PBS overnight at 4°C, followed by blocking with 2% bovine serum albumin (BSA) in PBS. Different dilutions (between 1:10<sup>3</sup> and 1:10<sup>8</sup>) of the sera from all of the immunized groups were prepared and coated in triplicate. After incubation at room temperature (RT) for 1 h, the plates were washed thrice with PBS-T. Horseradish peroxidase (HRP)-conjugated anti-mouse secondary antibodies (raised in goat; Santa Cruz Biotechnology) were added at 1:10,000 dilution and incubated at 37°C for 1 h. The plates were developed using OptEIA TMB substrate (BD Bioscience), and the absorbance was measured at 450 nm. The titers were determined by subtracting the background absorbance values of the uncoated wells from those of the coated wells. The threshold titer was determined as the mean of absorbance plus 3 times the standard deviation of a 1:100 dilution of the placebo group. The endpoint titer of the samples was defined as the inverse of the highest dilution with an absorbance (optical density at 450 nm) greater than that of the threshold value.

**Splenocyte culture.** Three weeks after the last immunization, 3 or 4 mice were sacrificed and the spleens were removed aseptically. Splenocytes were isolated as previously described (62). Briefly, the cells were suspended in complete RPMI medium and cultured in 96-well plates at  $1 \times 10^6$  cells/well. The cells were stimulated either with the test antigen (10  $\mu\text{g}$ ) or with 5  $\mu\text{g}$  of concanavalin A (ConA) as a positive inducer and cultured at 37°C under a humidified atmosphere of 5% CO<sub>2</sub>. The culture supernatant was collected after 72 h, aliquoted, and stored at -80°C until use.

**Cytokine measurements.** The levels of interleukin-4 (IL-4), tumor necrosis factor- $\alpha$  (TNF- $\alpha$ ), and gamma interferon (IFN- $\gamma$ ) were measured in the culture supernatant of stimulated splenocytes with BD OptEIA kits according to the manufacturer's protocol. The concentrations of the cytokine were calculated using a linear regression equation obtained from absorbance values of standards provided by the manufacturer.

In the protective efficacy experiment, the production of IL-2, IFN- $\gamma$ , TNF- $\alpha$ , IL-4, IL-6, IL-10, and IL-17A cytokines was measured in the culture supernatant using a BD cytometric bead array (CBA) mouse Th1/Th2/Th17 cytokine kit (BD Biosciences) according to the manufacturer's instructions. Whenever necessary, the samples were appropriately diluted before analysis. The data were acquired on a BD LSR II flow cytometer (Becton Dickinson) at the BD-JH FACS Academy, Jamia Hamdard, India, and analyzed using FCAP Array software, V3.0 (Becton Dickinson).

**Histopathological analysis.** Six weeks after the challenge with *M. tuberculosis*, the mice were dissected and the right lobe of the lung was excised under aseptic conditions, fixed in 10% (vol/vol) buffered formalin, embedded in paraffin blocks, and subjected to hematoxylin and eosin (H&E) staining. Granuloma formation was visualized and graded by a certified pathologist (blinded to the treatment of the groups) according to the criteria described previously by Kar et al. (63), and a score of 2.5 was assigned to each granuloma. The total granuloma score was obtained by adding up the marks of all the granulomas in each section of the lung.

**Protective efficacy.** From each group, four mice were sacrificed at 3 and 6 weeks postchallenge, and bacterial loads in the lung and spleen were recorded. Briefly, the lungs and spleen were removed aseptically, homogenized, serially diluted in sterile PBS, and plated on Middlebrook 7H10 agar plates containing oleic acid-albumin-dextrose-catalase supplements. The plates were then incubated at 37°C for 3 to 4 weeks and the colony count was enumerated. The protective efficacy was expressed as the inverse of the bacterial load in the organs of mice compared to that of the control. The results are expressed on the log<sub>10</sub> scale as reduction of bacterial counts in each immunized mouse group.

**Data representation and statistical analysis.** For data preparation and statistical analysis, Graph-Pad Prism v6.05 software was used. The results were represented as means  $\pm$  standard errors of means (SEM) of the data obtained from each immunized mouse group. In the dose optimization studies, for comparing the antibody titer data obtained from the antigen-alone group with an adjuvanted group, between two different adjuvanted groups, or between two different doses of the same adjuvanted group, *P* values were calculated using unpaired *t* test. For comparisons between multiple groups, one-way analysis of variance (ANOVA) followed by Tukey's multiple-comparison test was used. Log-rank Mantel-Cox tests were applied to calculate the significance of difference in the survival curve. Statistically significant differences are marked by asterisks in figures and explained in the figure legends: \*, *P* < 0.05; \*\*, *P* < 0.01; \*\*\*, *P* < 0.001; \*\*\*\*, *P* < 0.0001. The asterisks above the bars represent *P* values compared to antigen alone. The brackets at the top of the figure panels extend between test samples compared for statistical significance.

## SUPPLEMENTAL MATERIAL

Supplemental material for this article may be found at <https://doi.org/10.1128/IAI.00537-18>.

**SUPPLEMENTAL FILE 1**, PDF file, 0.3 MB.



## ACKNOWLEDGMENTS

We gratefully acknowledge the gas chromatography-mass spectrometry (GC-MS) and transmission electron microscopy (TEM) facilities of the Advanced Instrumentation Research Facility (AIRF), Jawaharlal Nehru University, New Delhi, India.

This work was financially supported by grants to N.B. and R.B. from the Department of Biotechnology, Ministry of Science and Technology (DBT), Government of India (BT/PR5540/MED/29/522/2012 and BT/55/NE/2017).

## REFERENCES

- World Health Organization. 2017. Global tuberculosis report 2017. World Health Organization, Geneva, Switzerland.
- Colditz GA, Brewer TF, Berkey CS, Wilson ME, Burdick E, Fineberg HV, Mosteller F. 1994. Efficacy of BCG vaccine in the prevention of tuberculosis: meta-analysis of the published literature. *JAMA* 271: 698–702. <https://doi.org/10.1001/jama.1994.03510330076038>.
- Manjelienskaia J, Erck D, Piracha S, Schragar L. 2016. Drug-resistant TB: deadly, costly and in need of a vaccine. *Trans R Soc Trop Med Hyg* 110:186–191. <https://doi.org/10.1093/trstmh/trw006>.
- Pasquale AD, Preiss S, Silva FTD, Garçon N. 2015. Vaccine adjuvants: from 1920 to 2015 and beyond. *Vaccines* 3:320–343. <https://doi.org/10.3390/vaccines3020320>.
- Reed SG, Orr MT, Fox CB. 2013. Key roles of adjuvants in modern vaccines. *Nat Med* 19:1597–1608. <https://doi.org/10.1038/nm.3409>.
- Vogel FR. 2000. Improving vaccine performance with adjuvants. *Clin Infect Dis* 30:S266–S270. <https://doi.org/10.1086/313883>.
- Awate S, Babiuk LAB, Mutwiri G. 2013. Mechanisms of action of adjuvants. *Front Immunol* 4:114. <https://doi.org/10.3389/fimmu.2013.00114>.
- Lee S, Nguyen MT. 2015. Recent advances of vaccine adjuvants for infectious diseases. *Immune Netw* 15:51–57. <https://doi.org/10.4110/in.2015.15.2.51>.
- HogenEsch H. 2002. Mechanisms of stimulation of the immune response by aluminum adjuvants. *Vaccine* 20:S34–S39. [https://doi.org/10.1016/S0264-410X\(02\)00169-X](https://doi.org/10.1016/S0264-410X(02)00169-X).
- O'Hagan DT. 2007. MF59 is a safe and potent vaccine adjuvant that enhances protection against influenza virus infection. *Expert Rev Vaccines* 6:699–710. <https://doi.org/10.1586/14760584.6.5.699>.
- Rosenkrands I, Agger EM, Olsen AW, Korsholm KS, Andersen CS, Jensen KT, Andersen P. 2005. Cationic liposomes containing mycobacterial lipids: a new powerful Th1 adjuvant system. *Infect Immun* 73:5817–5826. <https://doi.org/10.1128/IAI.73.9.5817-5826.2005>.
- Ottenhoff TH, Kaufmann SH. 2012. Vaccines against tuberculosis: where are we and where do we need to go? *PLoS Pathog* 8:e1002607. <https://doi.org/10.1371/journal.ppat.1002607>.
- Simon R, Tennant SM, Galen JE, Levine MM. 2011. Mouse models to assess the efficacy of non-typhoidal *Salmonella* vaccines: revisiting the role of host innate susceptibility and routes of challenge. *Vaccine* 29: 5094–5106. <https://doi.org/10.1016/j.vaccine.2011.05.022>.
- Clapp B, Skyberg JA, Yang X, Thornburg T, Walters N, Pascual DW. 2011. Protective live oral brucellosis vaccines stimulate Th1 and Th17 cell responses. *Infect Immun* 79:4165–4174. <https://doi.org/10.1128/IAI.05080-11>.
- Barber EM, Fazzari M, Pollard JW. 2005. Th1 cytokines are essential for placental immunity to *Listeria monocytogenes*. *Infect Immun* 73: 6322–6331. <https://doi.org/10.1128/IAI.73.10.6322-6331.2005>.
- Knudsen NPH, Olsen A, Buonsanti C, Follmann F, Zhang Y, Coler RN, Fox CB, Meinke A, Casini D, Bonci A. 2016. Different human vaccine adjuvants promote distinct antigen-independent immunological signatures tailored to different pathogens. *Sci Rep* 6:19570. <https://doi.org/10.1038/srep19570>.
- Aagaard C, Hoang T, Dietrich J, Cardona P-J, Izzo A, Dolganov G, Schoolnik GK, Cassidy JP, Billeskov R, Andersen P. 2011. A multistage tuberculosis vaccine that confers efficient protection before and after exposure. *Nat Med* 17:189. <https://doi.org/10.1038/nm.2285>.
- Jayashankar L, Hafner R. 2016. Adjunct strategies for tuberculosis vaccines: modulating key immune cell regulatory mechanisms to potentiate vaccination. *Front Immunol* 7:577. <https://doi.org/10.3389/fimmu.2016.00577>.
- Kaufmann SH, Weiner J, von Reyn CF. 2017. Novel approaches to tuberculosis vaccine development. *Int J Infect Dis* 56:263–267. <https://doi.org/10.1016/j.ijid.2016.10.018>.
- Agger EM, Rosenkrands I, Olsen AW, Hatch G, Williams A, Kritsch C, Lingnau K, Von Gabain A, Andersen CS, Korsholm KS. 2006. Protective immunity to tuberculosis with Ag85B-ESAT-6 in a synthetic cationic adjuvant system IC31. *Vaccine* 24:5452–5460. <https://doi.org/10.1016/j.vaccine.2006.03.072>.
- Doherty TM, Olsen AW, van Pinxteren L, Andersen P. 2002. Oral vaccination with subunit vaccines protects animals against aerosol infection with *Mycobacterium tuberculosis*. *Infect Immun* 70:3111–3121. <https://doi.org/10.1128/IAI.70.6.3111-3121.2002>.
- Holten-Andersen L, Doherty T, Korsholm K, Andersen P. 2004. Combination of the cationic surfactant dimethyl dioctadecyl ammonium bromide and synthetic mycobacterial cord factor as an efficient adjuvant for tuberculosis subunit vaccines. *Infect Immun* 72:1608–1617. <https://doi.org/10.1128/IAI.72.3.1608-1617.2004>.
- Azuma I, Kamisango K-I, Saiki I, Tanio Y, Kobayashi S, Yamamura Y. 1980. Adjuvant activity of N-acetyl muramyl dipeptides for the induction of delayed-type hypersensitivity to azobenzene arsonate-N-acetyl-L-tyrosine in guinea pigs. *Infect Immun* 29:1193–1196.
- Kasmar A, Layre E, Moody B. 2014. Lipid adjuvants and antigens embedded in the mycobacterial cell envelope, p 123–149. *In* Norazmi MN, Acosta A, Sarmiento ME (ed), *The art & science of tuberculosis vaccine development*, 2nd ed. Oxford University Press, Oxford, United Kingdom.
- Yonekawa A, Saijo S, Hoshino Y, Miyake Y, Ishikawa E, Suzukawa M, Inoue H, Tanaka M, Yoneyama M, Oh-Hora M. 2014. Dectin-2 is a direct receptor for mannose-capped lipoarabinomannan of mycobacteria. *Immunity* 41:402–413. <https://doi.org/10.1016/j.immuni.2014.08.005>.
- Kubota M, Iizasa H, Kiyohara H, Nakama Y, Hara H, Yoshida H. 2014. 207: *Mycobacterium tuberculosis*-derived mycolic acid shows an adjuvant activity by activation of the ITAM receptor/CARD9-mediated innate immunity. *Cytokine* 70:78. <https://doi.org/10.1016/j.cyto.2014.07.214>.
- Ostrop J, Jozefowski K, Zimmermann S, Hofmann K, Strasser E, Lepenies B, Lang R. 2015. Contribution of MINCLE-SYK signaling to activation of primary human APCs by mycobacterial cord factor and the novel adjuvant TDB. *J Immunol* 195:2417–2428. <https://doi.org/10.4049/jimmunol.1500102>.
- Rudra JS, Tian YF, Jung JP, Collier JH. 2010. A self-assembling peptide acting as an immune adjuvant. *Proc Natl Acad Sci U S A* 107:622–627. <https://doi.org/10.1073/pnas.0912124107>.
- Hirschfield GR, McNeil M, Brennan PJ. 1990. Peptidoglycan-associated polypeptides of *Mycobacterium tuberculosis*. *J Bacteriol* 172:1005–1013. <https://doi.org/10.1128/jb.172.2.1005-1013.1990>.
- Phiet P, Wietzerbin J, Zissman E, Petit J, Lederer E. 1976. Analysis of the cell wall of five strains of *Mycobacterium tuberculosis* BCG and of an attenuated human strain, W 115. *Infect Immun* 13:677–681.
- Wietzerbin J, Lederer F, Petit J-F. 1975. Structural study of the poly-L-glutamic acid of the cell wall of *Mycobacterium tuberculosis* var. hominis, strain Brevannes. *Biochem Biophys Res Commun* 62:246–252. [https://doi.org/10.1016/S0006-291X\(75\)80130-6](https://doi.org/10.1016/S0006-291X(75)80130-6).
- Wietzerbin-Falszpan J, Das BC, Gros C, Petit JF, Lederer E. 1973. The amino acids of the cell wall of *Mycobacterium tuberculosis* var. bovis, strain BCG: presence of a poly (L-glutamic acid). *Eur J Biochem* 32: 525–532. <https://doi.org/10.1111/j.1432-1033.1973.tb02637.x>.
- Harth G, Horwitz MA. 1999. An inhibitor of exported *Mycobacterium tuberculosis* glutamine synthetase selectively blocks the growth of pathogenic mycobacteria in axenic culture and in human monocytes: extracellular proteins as potential novel drug targets. *J Exp Med* 189: 1425–1436. <https://doi.org/10.1084/jem.189.9.1425>.
- Chandra H, Basir SF, Gupta M, Banerjee N. 2010. Glutamine synthetase encoded by *glnA-1* is necessary for cell wall resistance and pathogenicity

- of *Mycobacterium bovis*. *Microbiology* 156:3669–3677. <https://doi.org/10.1099/mic.0.043828-0>.
35. Garg R, Tripathi D, Kant S, Chandra H, Bhatnagar R, Banerjee N. 2015. The conserved hypothetical protein Rv0574c is required for cell wall integrity, stress tolerance, and virulence of *Mycobacterium tuberculosis*. *Infect Immun* 83:120–129. <https://doi.org/10.1128/IAI.02274-14>.
  36. McKee AS, Munks MW, Marrack P. 2007. How do adjuvants work? Important considerations for new generation adjuvants. *Immunity* 27:687–690. <https://doi.org/10.1016/j.immuni.2007.11.003>.
  37. Morel S, Didierlaurent A, Bourguignon P, Delhaye S, Baras B, Jacob V, Planty C, Elouahabi A, Harvengt P, Carlsen H. 2011. Adjuvant system AS03 containing  $\alpha$ -tocopherol modulates innate immune response and leads to improved adaptive immunity. *Vaccine* 29:2461–2473. <https://doi.org/10.1016/j.vaccine.2011.01.011>.
  38. Lindenstrøm T, Agger EM, Korsholm KS, Darrah PA, Aagaard C, Seder RA, Rosenkrands I, Andersen P. 2009. Tuberculosis subunit vaccination provides long-term protective immunity characterized by multifunctional CD4 memory T cells. *J Immunol* 182:8047–8055. <https://doi.org/10.4049/jimmunol.0801592>.
  39. Baldwin SL, Bertholet S, Reese VA, Ching LK, Reed SG, Coler RN. 2012. The importance of adjuvant formulation in the development of a tuberculosis vaccine. *J Immunol* 188:2189–2197. <https://doi.org/10.4049/jimmunol.1102696>.
  40. da Fonseca DM, Silva CL, Wowk PF, e Paula MO, Ramos SG, Horn C, Marchal G, Bonato VLD. 2009. *Mycobacterium tuberculosis* culture filtrate proteins plus CpG oligodeoxynucleotides confer protection to *Mycobacterium bovis* BCG-primed mice by inhibiting interleukin-4 secretion. *Infect Immun* 77:5311–5321. <https://doi.org/10.1128/IAI.00580-09>.
  41. Torrado E, Cooper AM. 2010. IL-17 and Th17 cells in tuberculosis. *Cytokine Growth Factor Rev* 21:455–462. <https://doi.org/10.1016/j.cytogfr.2010.10.004>.
  42. Lindenstrøm T, Woodworth J, Dietrich J, Aagaard C, Andersen P, Agger EM. 2012. Vaccine-induced th17 cells are maintained long-term postvaccination as a distinct and phenotypically stable memory subset. *Infect Immun* 80:3533–3544. <https://doi.org/10.1128/IAI.00550-12>.
  43. Dowling JK, Mansell A. 2016. Toll-like receptors: the Swiss army knife of immunity and vaccine development. *Clin Transl Immunol* 5:e85. <https://doi.org/10.1038/cti.2016.22>.
  44. Takahashi T, Katada S, Onodera O. 2010. Polyglutamine diseases: where does toxicity come from? What is toxicity? Where are we going? *J Mol Cell Biol* 2:180–191. <https://doi.org/10.1093/jmcb/mjq005>.
  45. Manish M, Rahi A, Kaur M, Bhatnagar R, Singh S. 2013. A single-dose PLGA encapsulated protective antigen domain 4 nanoformulation protects mice against *Bacillus anthracis* spore challenge. *PLoS One* 8:e61885. <https://doi.org/10.1371/journal.pone.0061885>.
  46. Branco LM, Grove JN, Geske FJ, Boisen ML, Muncy IJ, Magliato SA, Henderson LA, Schoepp RJ, Cashman KA, Hensley LE. 2010. Lassa virus-like particles displaying all major immunological determinants as a vaccine candidate for Lassa hemorrhagic fever. *Viol J* 7:279. <https://doi.org/10.1186/1743-422X-7-279>.
  47. Gao Y, Wijewardhana C, Mann JF. 2018. Virus-like particle, liposome, and polymeric particle-based vaccines against HIV-1. *Front Immunol* 9:345. <https://doi.org/10.3389/fimmu.2018.00345>.
  48. Sanders MT, Brown LE, Deliyannis G, Pearse MJ. 2005. ISCOMTM-based vaccines: the second decade. *Immunol Cell Biol* 83:119–128. <https://doi.org/10.1111/j.1440-1711.2005.01319.x>.
  49. Prados-Rosales R, Carreño L, Cheng T, Blanc C, Weinrick B, Malek A, Lowary TL, Baena A, Joe M, Bai Y. 2017. Enhanced control of *Mycobacterium tuberculosis* extrapulmonary dissemination in mice by an arabinomannan-protein conjugate vaccine. *PLoS Pathog* 13:e1006250. <https://doi.org/10.1371/journal.ppat.1006250>.
  50. Near KA, Stowers AW, Jankovic D, Kaslow DC. 2002. Improved immunogenicity and efficacy of the recombinant 19-kilodalton merozoite surface protein 1 by the addition of oligodeoxynucleotide and aluminum hydroxide gel in a murine malaria vaccine model. *Infect Immun* 70:692–701. <https://doi.org/10.1128/IAI.70.2.692-701.2002>.
  51. Thatte J, Rath S, Bal V. 1995. Analysis of immunization route-related variation in the immune response to heat-killed *Salmonella typhimurium* in mice. *Infect Immun* 63:99–103.
  52. Schmidt ST, Khadke S, Korsholm KS, Perrie Y, Rades T, Andersen P, Foged C, Christensen D. 2016. The administration route is decisive for the ability of the vaccine adjuvant CAF09 to induce antigen-specific CD8<sup>+</sup> T-cell responses: the immunological consequences of the biodistribution profile. *J Control Rel* 239:107–117. <https://doi.org/10.1016/j.jconrel.2016.08.034>.
  53. Rook GA, Hernández-Pando R, Zumla A. 2009. Tuberculosis due to high-dose challenge in partially immune individuals: a problem for vaccination? *J Infect Dis* 199(5):613–618. <https://doi.org/10.1086/596654>.
  54. Gupta M, Nayyar N, Chawla M, Sitaraman R, Bhatnagar R, Banerjee N. 2016. The chromosomal parDE2 toxin-antitoxin system of *Mycobacterium tuberculosis* H37Rv: genetic and functional characterization. *Front Microbiol* 7:886. <https://doi.org/10.3389/fmicb.2016.00886>.
  55. Masuko T, Minami A, Iwasaki N, Majima T, Nishimura S-I, Lee YC. 2005. Carbohydrate analysis by a phenol-sulfuric acid method in microplate format. *Anal Biochem* 339:69–72. <https://doi.org/10.1016/j.ab.2004.12.001>.
  56. Kruger NJ. 2002. The Bradford method for protein quantitation, p 15–21. *In Walker JM* (ed), *The protein protocols handbook*. Humana Press, New York, NY.
  57. Cheng YS, Zheng Y, VanderGheynst JS. 2011. Rapid quantitative analysis of lipids using a colorimetric method in a microplate format. *Lipids* 46:95–103. <https://doi.org/10.1007/s11745-010-3494-0>.
  58. De Mey M, Lequeux G, Maertens J, De Maeseineire S, Soetaert W, Vandamme E. 2006. Comparison of DNA and RNA quantification methods suitable for parameter estimation in metabolic modeling of microorganisms. *Anal Biochem* 353:198–203. <https://doi.org/10.1016/j.ab.2006.02.014>.
  59. Schägger H. 2006. Tricine-SDS-Page. *Nat Protoc* 1:16. <https://doi.org/10.1038/nprot.2006.4>.
  60. Gupta P, Waheed S, Bhatnagar R. 1999. Expression and purification of the recombinant protective antigen of *Bacillus anthracis*. *Protein Expr Purif* 16:369–376. <https://doi.org/10.1006/prep.1999.1066>.
  61. Singh J, Joshi MC, Bhatnagar R. 2004. Cloning and expression of mycobacterial glutamine synthetase gene in *Escherichia coli*. *Biochem Biophys Res Commun* 317:634–638. <https://doi.org/10.1016/j.bbrc.2004.03.094>.
  62. Malik A, Gupta M, Mani R, Gogoi H, Bhatnagar R. 2018. Trimethyl chitosan nanoparticles encapsulated protective antigen protects the mice against anthrax. *Front Immunol* 9:562. <https://doi.org/10.3389/fimmu.2018.00562>.
  63. Kar R, Nangpal P, Mathur S, Singh S, Tyagi AK. 2017. *bioA* mutant of *Mycobacterium tuberculosis* shows severe growth defect and imparts protection against tuberculosis in guinea pigs. *PLoS One* 12:e0179513. <https://doi.org/10.1371/journal.pone.0179513>.